J|A|C|S COMMUNICATIONS

Published on Web 10/26/2010

Guanine- and Potassium-Based Two-Dimensional Coordination Network Self-Assembled on Au(111)

Wei Xu,*[,†,‡] Jian-guo Wang,[§] Miao Yu,[†] Erik Lægsgaard,[†] Ivan Stensgaard,[†] Trolle R. Linderoth,[†] Bjørk Hammer,[†] Chen Wang,[||] and Flemming Besenbacher*[,†]

Interdisciplinary Nanoscience Center (iNANO), Center for DNA Nanotechnology (CDNA), and Department of Physics and Astronomy, University of Aarhus, Ny Munkegade, DK 8000 Aarhus C, Denmark, College of Materials Science and Engineering, Tongji University, 4800 Cao An Road, Shanghai 201804, P. R. China, Institute of Industrial Catalysis, College of Chemical Engineering and Materials Science, Zhejiang University of Technology, Hangzhou 310032, P. R. China, and National Center for Nanoscience and Technology, Beijing 100190, P. R. China

Received September 1, 2010; E-mail: xuwei@tongji.edu.cn; fbe@inano.au.dk

Abstract: In this study, through the choice of the well-known G−K biological coordination system, bioligand−alkali metal coordination has for the first time been brought onto an inert Au(111) surface. Using the interplay between high-resolution scanning tunneling microscopy and density functional theory calculations, we show that the mobile G molecules on Au(111) can effectively coordinate with the K atoms, resulting in a metallosupramolecular porous network that is stabilized by a delicate balance between hydrogen bonding and metal−organic coordination.

The synthesis of desired molecular architectures on surfaces by bottom-up self-assembly and directed-assembly processes is one of the challenging goals within the rapidly developing field of nanoscience and nanotechnology.[1−4] The intermolecular forces at play in self-assembly of surface molecular nanostructures cover the entire range from weak noncovalent interactions (e.g., hydrogen bonding) to strong covalent bonding directly synthesized on the surfaces.[5,6] In particular, metal−ligand bonding known from organometallic and coordination chemistry has been extensively employed by the surface science community to grow highly ordered supramolecular surface nanostructures in which transition metals such as Fe, Co, Ni, an Cu are involved as the main metal sources.[7−14] To date, bioorganometallic chemistry has mainly focused on the full three-dimensional structural aspects of complexes that contain bioligands, and significant advances in characterizing structural diversity and understanding molecular recognition processes have been made.[15] In the present communication, however, we demonstrate that it is possible to bring the concepts of bioorganometallic chemistry onto two-dimensional (2D) surfaces, thereby allowing the exploration of some of the biologically relevant issues using surface science tools and in particular the directly visualization of such structures.

Alkali metals, specifically Na and K, are known to play a vital role in several cellular environments. As an example of an important biological system, guanine (G) quadruplexes coordinated with either Na or K in human telomeric DNA have elicited fundamental interest in different disciplines because of the potential applications for novel anticancer drug design.[16−18] Here we studied the G−K bioligand−alkali metal coordination system on a 2D Au(111) surface under ultrahigh vacuum (UHV) conditions. Using the interplay between high-resolution scanning tunneling microscopy (STM) and density functional theory (DFT) calculations, we show that mobile G molecules on the Au(111) surface can coordinate with K atoms, resulting in the formation of a metallosupramolecular porous network that is stabilized by a delicate balance between hydrogen bonding and metal−organic coordination. This metallosupramolecular network structure represents a model system that allows us to explore the fundamental coordination between G molecules and K atoms at the atomic scale with the aim of identifying binding sites that are the key to the structural and catalytical properties of bioorganometallic complexes.

The experiments were performed in a UHV chamber equipped with a variable-temperature Aarhus scanning tunneling microscope.[19] The single-crystal Au(111) sample was prepared using standard procedures.[20] The G molecules were loaded into a glass crucible that was mounted in the molecular evaporator. After the system was thoroughly degassed, the G molecules were first deposited by thermal sublimation at 420 K onto a clean Au(111) substrate held at room temperature (RT). The K atoms were subsequently deposited onto the G-covered surface at RT. The sample was thereafter transferred within the UHV chamber to the scanning tunneling microscope, where measurements were carried out over a temperature range of 120−150 K to stabilize the formed nanostructures. The DFT calculations were performed with the DACAPO code employing plane waves and ultrasoft pseudopotentials.

The STM results revealed that sequential codeposition of G molecules and K atoms led to the formation of a porous network, as depicted in Figure 1A; this was found to coexist with G-quartet-based coordination networks (discussed elsewhere in our unpublished results). This G−K porous network, which is dramatically different from the previously reported G-quartet network,[21,22] must be associated with the deposition of K atoms. We have previously shown that individual G molecules on Au(111) appear in the STM images as triangular protrusions,[21,22] and from Figure 1A we conclude that the porous network (with islands 50 nm across on average) consists of G *dimers* (schematically indicated in Figure S1 in the Supporting Information) that are regularly distributed and linked together. Under certain tip conditions [Figure 1C (left panel) and Figure 2A], high-resolution STM images were obtained in which round-shaped, atomic-sized extra features in the porous network were resolved. These features have been assigned to individual K atoms. A detailed analysis of the STM images revealed that the G−K network is chiral, since some of the G dimers face upward while others face downward (see the enlarged high-resolution STM image in the Supporting Information). In fact,

[†] University of Aarhus.
[‡] Tongji University.
[§] Zhejiang University of Technology.
[||] National Center for Nanoscience and Technology.

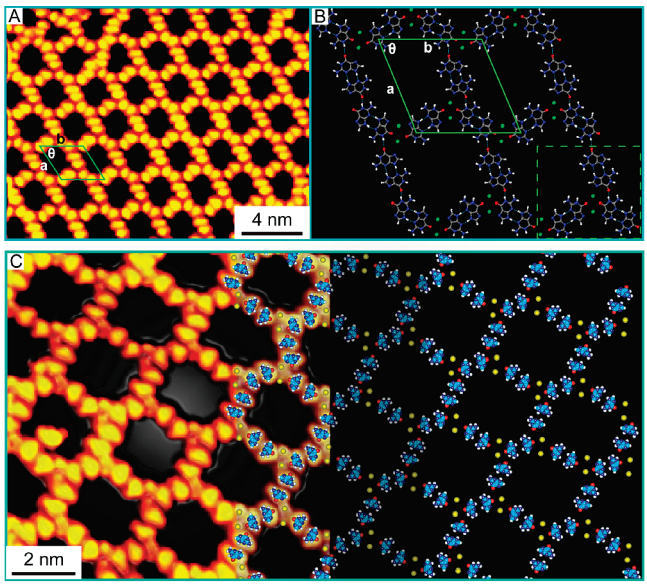

Figure 1. STM images and DFT models of the G−K porous network. (A) High-resolution STM image of the ordered G−K network. (B) DFT model of the G−K network with K atoms indicated as green spots. The indicated unit cell has parameters $a = 25.5$ Å, $b = 26.5$ Å, $\theta = 67°$. The dashed box indicates the elementary building block. (C) High-resolution STM image revealing bright spots where K atoms are believed to be. The theoretical model is partially superimposed. The experimental unit cell has parameters $a = 25 \pm 0.5$ Å, $b = 27 \pm 0.5$ Å, $\theta = 65 \pm 1°$. Scanning conditions: (A) $I_t = -0.96$ nA, $V_t = -1486$ mV; (C) $I_t = -0.92$ nA, $V_t = -1250$ mV.

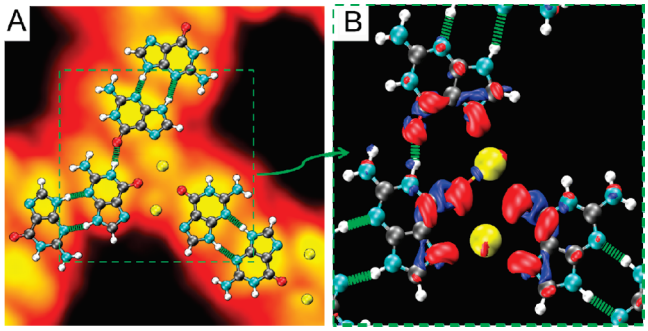

Figure 2. (A) The elementary building block including three G dimers and two K dimers is superimposed on the high-resolution STM image. Hydrogen bonds are indicated by the green lines. (B) The cutoff of charge density difference between the three G dimers and the two K dimers at the level of 0.015 e Å^{-3}. Blue and red isosurfaces indicate charge depletion and addition, respectively.

Figure 1A,C show images of two different chiral forms of the G−K porous network that were recorded within the same experiment.

To support the structural assignments based on the STM images, an extensive structural search for the most stable G−K structure was performed using DFT. Here, the number of K atoms and the geometries of the intermolecular G−G and G−K coordinations were varied. The resulting gas-phase model depicted in Figures 1B, 1C (right panel), and 2 fully corroborates the experimental findings. The formation energy of the network relative to isolated G molecules and dimers of K atoms was calculated to be 1.24 eV per G, implying that it is even more stable than the previously reported G-quartet network (1.10 eV per G).[21,22]

To extract information on the physiochemical nature of the formation mechanism and more specifically to identify the contributions of hydrogen bonding and metal−ligand interactions, a charge density difference analysis based on the elementary building block indicated in Figure 2 was performed. This building block, which contains three G dimers and two K dimers, is superimposed on the high-resolution STM image in Figure 2A. In Figure 2B, a zoomed-in view of the total charge density minus the sum of the charges of the three G dimers and the two K dimers in the unit cell is shown. The red isosurfaces appearing on the carbonyl functions and the N atoms facing the K atoms provide evidence of the metal−ligand interactions. Similarly, the red isosurfaces on the carbonyl functions facing N functions (i.e., the ones *not* adjacent to the K atoms) provide evidence of polarization and hence strengthening of the hydrogen bonding between the two G dimers. Since the hydrogen bonding is enhanced upon the introduction of the metal−ligand bonding, we thus conclude that the formation of the porous G−K network results from cooperative effects involving both kinds of interactions.

We note that since the G molecules are heterochiral within the porous network, it is unlikely that the network forms from interdiffusion of K atoms into any (homochiral) G-quartet networks formed before the introduction of K. Rather, we propose the following scenario: (i) After deposition on Au(111) at RT, some G molecules form the well-known G-quartet network,[21,22] whereas a racemic mixture of G molecules behaves as a 2D gas. (ii) After deposition of K atoms, the highly mobile G molecules within the 2D gas are trapped by the K atoms through the cooperative metal−ligand and hydrogen-bonding interactions, resulting in the formation of the observed porous network upon cooling to low temperature (∼120 K). The DFT calculations support this scheme, as calculations on several small G−K coordination clusters revealed that these G−K clusters have increased stability in comparison with the G clusters alone (e.g., G dimers, G trimers, G quartets).

In summary, we have demonstrated using STM that a bioligand−alkali metal coordination network is formed when G and K are deposited on an inert Au(111) surface, and using the interplay between the STM results and DFT calculations, we have identified the atomic-scale structure and especially the coordination binding sites. Additional experiments involving the codeposition of Na and G are currently underway to reveal the difference between the coordination configurations of K and Na with respect to G. Such a model system would provide new insight into the basic physiochemical nature of biologically relevant systems.

Acknowledgment. We acknowledge financial support from the Danish Ministry for Science, Technology, and Innovation through the iNANO Center, the Danish National Research Foundation, the Danish Research Councils, the Carlsberg Foundation, the Villum Kahn Rasmussen Foundation, the Danish Center for Scientific Computing, the New Century Excellent Talents in University Program (NCET-10-0607 to W.X.), the National Natural Science Foundation of China (20906081 to J.-g.W.), and the ERC. Zheshen Li is acknowledged for providing the K source.

Supporting Information Available: An enlarged high-resolution STM image of the G−K coordination network, a charge difference map, and a description of the theoretical method. This material is available free of charge via the Internet at http://pubs.acs.org.

References

(1) Barth, J. V.; Costantini, G.; Kern, K. *Nature* **2005**, *437*, 671.
(2) Otero, R.; Rosei, F.; Besenbacher, F. *Annu. Rev. Phys. Chem.* **2006**, *57*, 497.
(3) Wan, L. J. *Acc. Chem. Res.* **2006**, *39*, 334.
(4) De Feyter, S.; De Schryver, F. C. *Chem. Soc. Rev.* **2003**, *32*, 139.
(5) Weigelt, S.; Schnadt, J.; Tuxen, A.; Masini, F.; Bombis, C.; Busse, C.; Isvoranu, C.; Ataman, E.; Lægsgaard, E.; Besenbacher, F.; Linderoth, T. R. *J. Am. Chem. Soc.* **2008**, *130*, 5388.
(6) Weigelt, S.; Bombis, C.; Busse, C.; Knudsen, M. M.; Gothelf, K. V.; Lægsgaard, E.; Besenbacher, F.; Linderoth, T. R. *ACS Nano* **2008**, *2*, 651.

(7) Stepanow, S.; Lingenfelder, M.; Dmitriev, A.; Spillmann, H.; Delvigne, E.; Lin, N.; Deng, X.; Cai, C.; Barth, J. V.; Kern, K. *Nat. Mater.* **2004**, *3*, 229.
(8) Shi, Z.; Lin, N. *J. Am. Chem. Soc.* **2009**, *131*, 5376.
(9) Tait, S. L.; Wang, Y.; Costantini, G.; Lin, N.; Baraldi, A.; Esch, F.; Petaccia, L.; Lizzit, S.; Kern, K. *J. Am. Chem. Soc.* **2008**, *130*, 2108.
(10) Messina, P.; Dmitriev, A.; Lin, N.; Spillmann, H.; Abel, M.; Barth, J. V.; Kern, K. *J. Am. Chem. Soc.* **2002**, *124*, 14000.
(11) Lin, N.; Dmitriev, A.; Weckesser, J.; Barth, J. V.; Kern, K. *Angew. Chem., Int. Ed.* **2002**, *41*, 4779.
(12) Langner, A.; Tait, S. L.; Lin, N.; Rajadurai, C.; Ruben, M.; Kern, K. *Angew. Chem., Int. Ed.* **2008**, *47*, 8835.
(13) Björk, J.; Matena, M.; Dyer, M. S.; Enache, M.; Lobo-Checa, J.; Gade, L. H.; Jung, T. A.; Stöhr, M.; Persson, M. *Phys. Chem. Chem. Phys.* **2010**, *12*, 8815.
(14) Maksymovych, P.; Yates, J. T., Jr. *J. Am. Chem. Soc.* **2008**, *13*, 7518.
(15) Fish, R. H.; Jaouen, G. *Organometallics* **2003**, *22*, 2166.
(16) Hurley, L. H. *Nat. Rev. Cancer* **2002**, *2*, 188.
(17) Neidle, S.; Parkinson, G. *Nat. Rev. Drug Discovery* **2002**, *1*, 383.
(18) Davis, J. T. *Angew. Chem., Int. Ed.* **2004**, *43*, 668.
(19) Laegsgaard, E.; Osterlund, L.; Thostrup, P.; Rasmussen, P. B.; Stensgaard, I.; Besenbacher, F. *Rev. Sci. Instrum.* **2001**, *72*, 3537.
(20) Barth, J. V.; Brune, H.; Ertl, G.; Behm, R. J. *Phys. Rev. B* **1990**, *42*, 9307.
(21) Otero, R.; Schock, M.; Molina, L. M.; Lægsgaard, E.; Stensgaard, I.; Hammer, B.; Besenbacher, F. *Angew. Chem., Int. Ed.* **2005**, *44*, 2270.
(22) Xu, W.; Kelly, R. E. A.; Gersen, H.; Lægsgaard, E.; Stensgaard, I.; Kantorovich, L. N.; Besenbacher, F. *Small* **2009**, *5*, 1952.

JA1078909